

THERMAL MECHANICAL FATIGUE OF A 56 I/O PLASTIC QUAD-FLAT NOLEAD (PQFN) PACKAGE

Paul Vianco, Ph.D., and Michael K Neilsen, Ph.D.

Sandia National Laboratories

Albuquerque, NM, USA

ptvianc@sandia.gov, mkneils@sandia.gov

ABSTRACT

High reliability systems are using commercial electronics supply chain for providing advanced packages that meet reduced size, weight, and power (SWaP) goals as well as provide adequate, second-level interconnection reliability. The Sandia solder fatigue computational model was used to predict the effects of conformal coating and underfill on the thermal mechanical fatigue (TMF) reliability of 63Sn-37Pb (wt.%) solder joints formed between a 56 I/O plastic quad-flat (package), no-lead (PQFN) component and polyimide glass printed circuit board (PCB). The analysis included a 24 I/O leadless ceramic chip carrier (LCCC) package of similar footprint size. An accelerated aging thermal cycle was used having temperature limits of -55°C and 85°C. Two failure criteria were employed: (a) cycles to crack initiation and (b) cycles to cause 100% cracking (electrical open) of a solder joint. As expected, the LCCC experienced a considerably shorter baseline TMF lifetime than did the PQFN. Placing a conformal coating over the PWA reduced the TMF lifetime of both components in similar proportions to their baseline values. Having the conformal coating flow into the package/PCB gap caused a precipitous drop of TMF lifetime to similar metrics for both package types. The lower lifetimes reflected the significant conformal coat pressure pushing up on the packages. The introduction of the underfill material not only prevented the incursion of conformal coating under the package, but also enhanced the TMF lifetimes of both packages above their baseline values. The presence of 30% voids in the paddle joint of the PQFN had negligible effect on the TMF lifetimes of the peripheral solder interconnections.

Key words: solder, fatigue, conformal coat, underfill, PQFN.

INTRODUCTION

Electronics are an important enabler for high-reliability systems in military, space, and satellite hardware to meet operational objectives. High reliability hardware is constrained by the need to meet stringent size, weight, and power (SWaP) requirements. Therefore, advantage is taken, whenever possible, of the further miniaturization and increased functionality found in advanced electronic packages. Moreover, the continued diminishment of

captured manufacturing capabilities has forced the high-reliability electronic community to rely upon the commercial electronics supply chain for critical components and sub-systems. The plastic quad-flat package, no-leads (PQFN) is one packaging configuration that is filling both miniaturization as well as functionality goals by replacing small outline components as well as the traditional leadless ceramic chip carrier (LCCC) packages in high-reliability systems.

The high-reliability electronics community is faced with the challenge to understand the *long-term performance of second-level interconnections* made between these advanced packages and the underlying printed circuit board (PCB). Budget constraints and protracted development cycles, as well as the growing variety of new materials and use environments, have made it nearly impossible to develop thorough reliability data that are based solely on empirical programs. The alternative approach has been to construct computational models that predict the reliability of second-level interconnections with a fidelity that is sufficient to support design and manufacturing decisions under mounting program constraints.

One such application in which Sandia National Laboratories has taken the “modeling approach” is to understand the reliability of PQFN solder joints when the package and associated PCB are covered with conformal coatings or have underfill materials placed between them and the PCB. The printed wiring assemblies (PWAs) of high-reliability electronics are often covered with a thin, (0.127 mm), rubbery conformal coating to protect them from harsh environments that include dirt, organic growth, and handling damage. Larger surface mount components are also underfilled prior to conformal coating for shock and vibration protection. Underfill materials are typically epoxies which are highly filled with particles of aluminum oxide or silicon oxide in order to tailor their coefficients of thermal expansion (CTE) to more closely match those of the component, solder joints, and printed circuit board (PCB). Given the variety of both conformal coating and underfill products, as well as applications that use different varieties of PCBs, empirical studies were not a viable approach to develop the requisite solder joint reliability information. Therefore, the Sandia solder fatigue computation model was

used to predict the reliability of interconnections in the company of conformal coatings and underfills.

PREDICTIVE MODEL DEVELOPMENT

Computational modeling analyses were performed to predict the effects of conformal coat and underfill on the thermal mechanical fatigue (TMF) life of the solder interconnects for two package types: (a) baseline 8.89 x 8.89 mm, 24 I/O Leadless Ceramic Chip (LCCC) package and (b) the replacement package, an 8.0 x 8.0 mm, 56 I/O plastic quad flat no-lead (PQFN) geometry. Models of the packages and their interconnection structures are shown in Figure 1. The parts were soldered to a 2.36 mm thick polyimide glass PCB.

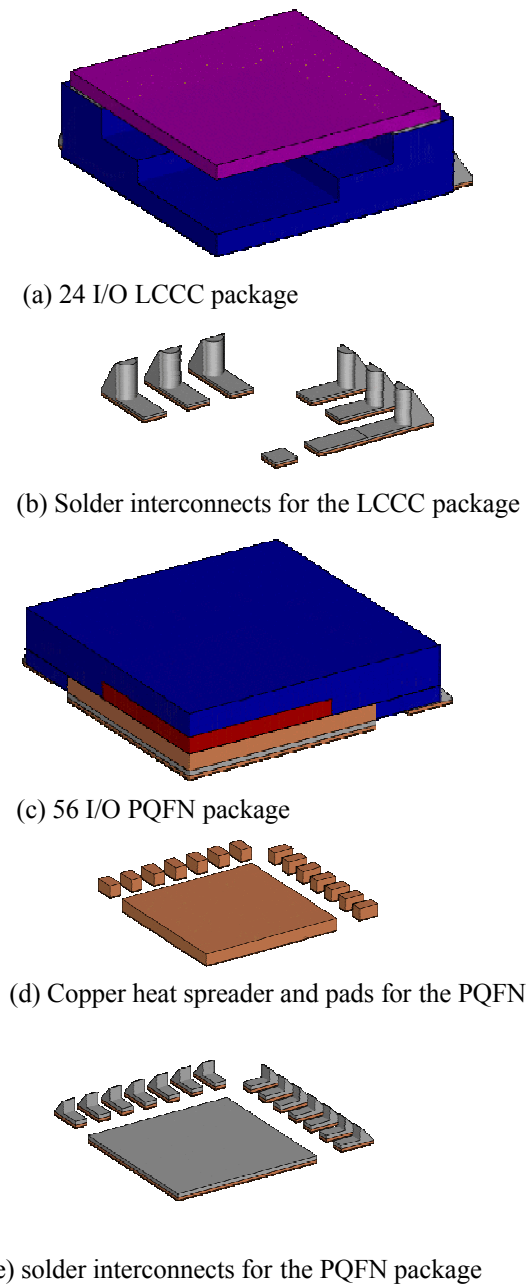


Figure 1. Models of $\frac{1}{4}$ of PQFN and LCCC packages

Finite element analyses were performed using models shown in Figure 2. These models represent one quarter of a 56 I/O PQFN or 24 I/O LCCC soldered to the PCB (green) with eutectic 63Sn-37Pb (wt.%) solder (gray). The other structures are: copper pads (copper), package (blue), LCCC lid (magenta), silicon (Si) die (red), conformal coat (yellow), and material in the gap, whether conformal coating or underfill (magenta). For both packages, the conformal coating above the package had a nominal thickness of 0.127 mm.

The first simulations were the baseline condition whereby the conformal coat and underfill were absent from the model. In the second simulation, the yellow conformal coating covered the packages and surface of the PCB; but, the space was empty under the package. The third simulation had the “magenta material,” which in this case was conformal coating, put under the package. In the fourth and final simulation, the magenta material under the package was given the properties of a typical underfill agent.

The occurrence of voids in the paddle solder joint has been a concern of both design and process engineers tasked with the use of the PQFN. Given the increased miniaturization and functionality of PQFN packages, they tend to generate significant heat loads that require heat dissipation that is provided by the paddle solder joint. Thermal efficiency is maximized by minimizing the degree of void formation in that joint. Unfortunately, these voids are difficult to mitigate because of the large areal footprint of the paddle. Regardless of the thermal management concerns or process challenges, it is not well established whether the presence of voids impact the TMF resistance of, not only the paddle joint, but also the reliability of the peripheral joints. Therefore, the four PQFN simulations were repeated, using a paddle solder interconnection having a relatively significant void presence of 30 percent by area of the joint footprint. The solid model of this condition is shown in Figure 2g. The voids each had similar size, but were randomly distributed through the joint. It was assumed that the void volume reached both the Cu paddle and PCB Cu pad surfaces – that is, they were not entirely internal to the solder layer. This geometry was used because paddle joint voids are typically due to (a) an inadequate amount of solder or (b) poor solder wetting and spreading. Both conditions lead to this variant of void configuration, which is the most detrimental to removing heat from the die.

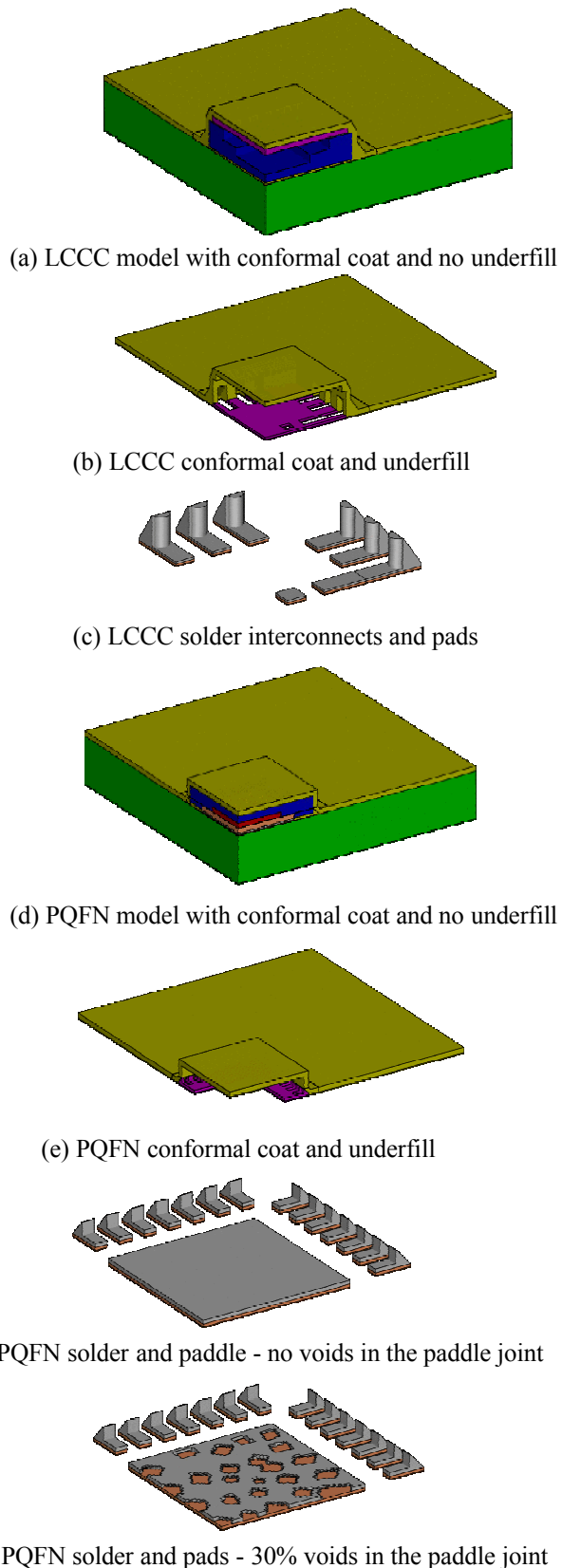


Figure 2. Finite Element Models of $\frac{1}{4}$ of PQFN and LCCC packages with variations in conformal coat and underfill.

Material properties used in these analyses are given in Tables 1 to 3, and Figure 3. The following structures were modeled as isotropic linear elastic materials with the material parameters listed in Table 1: copper pads, ceramic LCCC package, package lid, 80Au20Sn solder used to attach the lid to the ceramic, PQFN molding, PQFN die, and conformal coat. The conformal coat is rubbery at room temperature and was assumed to be temperature dependent, linear elastic with a variation in Young's Modulus and Bulk Modulus versus temperature as shown in Figure 3. The underfill is glassy at room temperature; but, its properties vary with temperature as shown in Figure 3. A unified creep plasticity damage (UCPD) model [1] was used for the solder with parameters listed in Table 2. The polyimide-glass printed circuit board was modeled as an orthotropic elastic material with the parameters listed in Table 3.

It is noted in Tables 1 to 3 that singular values are used for coefficients of thermal expansion (CTE). This approximation is suitable for the temperature range used in the thermal cycle.

Table 1. Properties for elastic materials.

Material	Young's Modulus (MPa)	Poisson's Ratio	Coefficient of Thermal Expansion ($1/^\circ\text{C}$)
Copper	117,241	0.350	17.50×10^{-6}
PQFN Die	184,828	0.278	2.80×10^{-6}
PQFN Molding	27,000	0.350	8.00×10^{-6}
LCCC ceramic	282,759	0.210	6.67×10^{-6}
LCCC lid	139,310	0.346	5.40×10^{-6}
LCCC lid solder	59,310	0.405	15.88×10^{-6}
Conformal Coat*	28.0	0.497667	222.0×10^{-6}
Underfill*	7,695	0.350	38.00×10^{-6}

* at room temperature, variation w/ temperature in Figure 3.

Table 2. UCPD material parameters for 63Sn-37Pb solder.

Temperature ($^\circ\text{C}$)	-60.0	21.0	100.0
Young's Modulus (MPa)	48,276	43,255	36,860
Poisson's Ratio	0.38	0.39	0.40
CTE ($1/^\circ\text{C}$)	25.0×10^{-6}		
Flow Rate, f	4.14×10^{-20}	1.88×10^{-9}	2.21×10^{-5}
Sinh Exponent - p	7.1778	4.2074	3.7151
Iso. Hard. (MPa^{A3+1})	270.67	193.44	167.76
Iso. Recov. ($1/\text{MPa}\cdot\text{sec}$)	0.379×10^{-3}	1.81×10^{-3}	8.31×10^{-3}
Iso. Exponent	0.970	0.970	0.970
Kin. Hard. (MPa^{A6+1})	0.0		
Kin. Recov. ($1/\text{MPa}\cdot\text{sec}$)	0.0		
Kin. Exponent	0.0		
Flow Stress - D_0 (MPa)	8.2759		
Damage Param. - a	1.31636		
Damage Param. - b	1.96078		
Damage Param. - c	0.250		

Table 3. Properties for orthotropic printed circuit board.

Parameter	Value
Young's Modulus XX, ZZ (MPa)	22,069
Young's Modulus YY (MPa)	5,517
Poisson's Ratio YX	0.0234
Poisson's Ratio ZX	0.150
Poisson's Ratio ZY	0.380
Shear Modulus XY (MPa)	5,545
Shear Modulus YZ (MPa)	5,545
Shear Modulus ZX (MPa)	9,593
CTE XX,ZZ (1/°C)	17.0 x 10 ⁻⁶
CTE YY (1/°C)	55.0 x 10 ⁻⁶

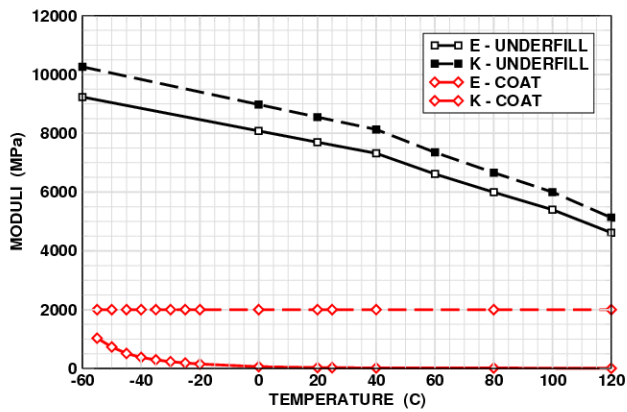


Figure 3. Young's modulus, E, and bulk modulus, K, for underfill and conformal coating as a function of temperature.

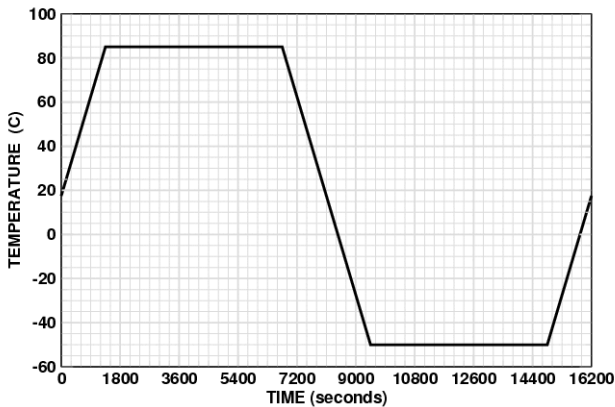


Figure 4. Accelerated aging cycle: 90 minute holds, temperature minimum -50°C; temperature maximum, 85°C.

In the first series of analyses, the models in Figure 2 were subjected to the -50 to 85 °C accelerated aging temperature cycle shown in Figure 4. The Coffin-Manson criterion was used for establishing the point of crack initiation in the eutectic Sn-Pb solder [2]. Under this criterion, the number

of cycles to “failure”, N_f , is a function of plastic shear strain range, $\Delta\gamma_p$, or the equivalent plastic strain (EQPS) from a single complete cycle, $\Delta EQPS$, as shown in Equation (1):

$$N_f = \left(\frac{1.14}{\Delta\gamma_p} \right)^{\frac{1}{0.51}} = \left(\frac{1.31636}{\Delta EQPS} \right)^{1.96078} \quad (1)$$

The maximum equivalent plastic strain increment from the finite element simulations was used to generate predictions for cycles needed to start a fatigue crack based on Equation (1). The UCPD model was then used to generate predictions for cycles needed to grow the fatigue crack to 100%, that is, an electrical open.

ANALYSIS OF MODEL PREDICTIONS

LCCC package predictions

The assessment begins with examining the predictions in Figure 5. A comparison of Figure 5a with Figure 5b shows that the already few cycles to start a fatigue crack in the baseline condition (Figure 5a) will be further reduced by the addition of the 0.127mm thick top conformal coat. In both cases, the interconnection experiencing the greatest extent of TMF are at the corners. This observation corroborates the fact that these joints are the furthest distance from the neutral point (DNP). Crack initiation begins at the junction between the fillet and the gap, as expected, when shear deformation predominates the fatigue behavior. This fatigue map corroborates the concept that, when the conformal coating is adherent, or coupled, to the PCB, its high thermal expansion coefficient causes the PCB to have a higher *effective* CTE value. The stiff, ceramic package of the LCCC is not affected by the conformal coating on it. Therefore, the net effect is an increase in the shear deformation mode to the solder joints.

A comparison of Figure 5c with Figures 5a and 5b shows that, not only is the lifetime dramatically reduced if the conformal coat is allowed to flow under the LCCC, but there is also a significant change to the TMF pattern in the interconnections. First of all, the location of greatest TMF deformation is at the inside edge of the solder joints. Secondly, all of the solder joints, not simply the corner interconnections with the greatest DNP, experienced similar TMF degradation. This observation indicates that the predominant TMF deformation contributing to the EQPS has changed from primarily a shear load due to global (package/PCB) thermal expansion mismatch to a tensile/compressive load in the vertical (YY) direction. Specifically, the conformal coating is attempting to push the LCCC package away and then pull it back towards the PCB surface. The TMF strain is distributed evenly amongst all of the solder interconnections under this loading condition.

Next, a comparison is made between Figures 5a – 5c and Figure 5d. In the latter case, an underfill was put under the package prior to the conformal coating, which prevents that latter from flowing between the package and PCB. Addition

of underfill which keeps conformal coating out from under the package dramatically improved TMF lifetime. In fact, the underfill was predicted to increase the number of cycles needed to start a fatigue crack *above* the baseline condition; that is, the underfill also directly improved the TMF lifetime of the interconnections. The TMF in Figure 5d had returned to primarily a shear deformation. The minimal CTE difference between the underfill (38 ppm/ $^{\circ}$ C) and solder (25 ppm/ $^{\circ}$ C), together with the low modulus of the underfill material, minimized the underfill pressure that would push the package up, off of the PCB. Therefore, the underfill prevented, not only the deleterious effects of conformal coating under the package and lifting it off of the PCB, but it also reduced the effective CTE mismatch between the LCCC and PCB by bonding the two structures together. The result was net *increase* in the TMF lifetime over the baseline conditions.

The predictions for cycles needed to generate a 100% TMF crack through an interconnection that gives rise to an electrical open, are shown in Figure 6. The white regions indicate cracked elements. The contour LIFE is equal to the damage divide by critical damage. A value of zero represents undamaged solder and a value of one represents solder with a fatigue crack. The baseline case is shown in Figure 6a. The cracks responsible for a 100% electrical open, passed along the fillet/pad interface, from the package corner where they initiated (Figure 5a), to the fillet toe. But, cracking had also initiated, and progressed some distance from the inner edge of the gap. Although the latter cracks did not cause the electrical open, they readily illustrate the gradient in TMF degradation from being greatest at the corner interconnections and decreasing away from them. These trends mirror those observed in Figure 5a.

Incidentally, the comparison between Figures 5a and 6a show the significant contribution of TMF crack *propagation* to the overall fatigue lifetime of the interconnections. The cycles required to start a crack accounted for only 18% of that lifetime. This comparison illustrates the value of having a capability to predict TMF crack propagation (i.e., the UCPD model) towards the development of a design tool for PWA reliability.

A second, interesting behavior was observed at the start of the analyses described in Figure 6. When a comparison is made between Figures 5a and 5b, the presence of the conformal coating on top of the component (the package/PCB gap was empty – a void) caused the cycles to TMF crack initiation to decrease from 190 cycles to 114 cycles, which is a drop of approximately 40%. However, in the case of TMF crack propagation, by subtracting out the cycles to crack initiation from the respective 100% crack cycles in Figures 6a and 6b, the net difference in crack propagation is 55% between baseline and conformal coating cases. This analysis illustrates the fact that crack propagation does not necessarily scale with the cycles required to reach crack initiation.

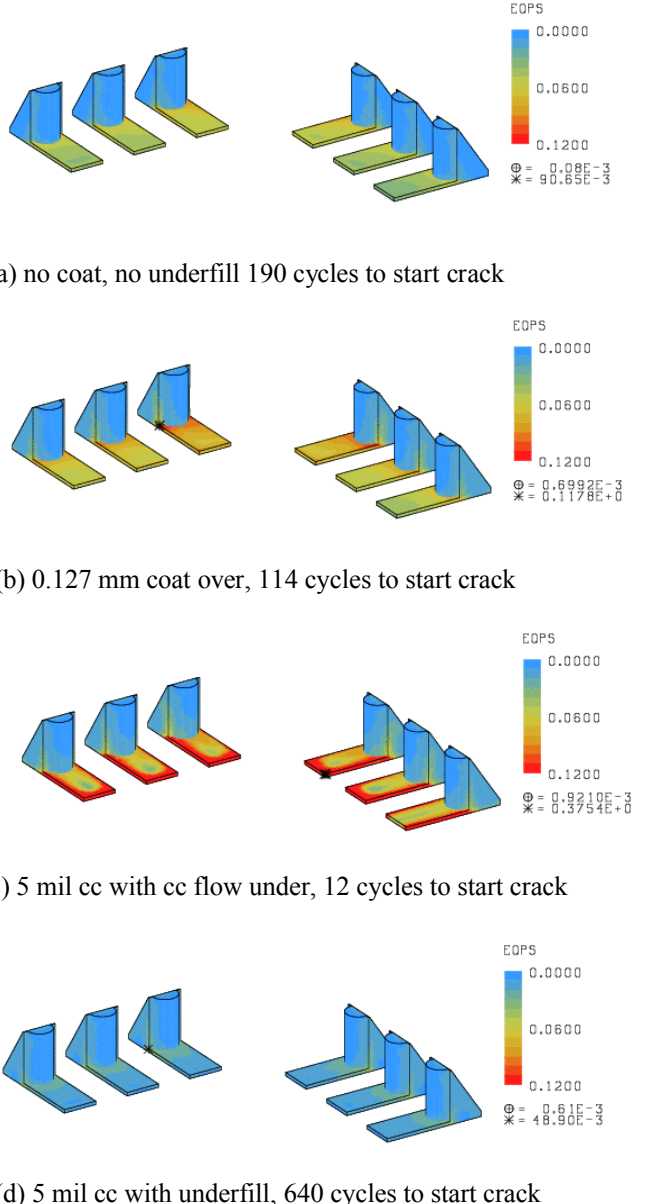


Figure 5. Predicted solder Δ EQPS for 24 I/O LCCC

As anticipated from the discussion of Fig. 5c, the presence of conformal coating material under the component significantly reduced the cycles to failure (Figure 6c) from 1020 cycles to 270 cycles. The cracked elements (white) were located in the solder gap. This pattern was the same for all of the joints, indicating once again, conformal coat pushing the component away from and then pulling it back towards the PCB surface was responsible for the 100% crack condition.

Lastly, contours in Figure 6d confirmed that preventing the entry of conformal coat between the package and PCB increased the TMF cycles required to reach an electrical open. The cycles increased by nearly three-fold compared

to the baseline condition; the same multiplying factor was observed for the crack initiation data.

Although the TMF crack propagation initiated at the corner of the package, it propagated to approximately equal extents in *both directions*, that is from the package corner to the fillet toe, and from the corner to the inside gap edge. The slightly faster crack growth to the fillet toe was ultimately responsible for the open. Aside from extending the TMF lifetime of LCCC solder joints against accelerated degradation by conformal coating in the gap, underfill provides the means to further increase the fatigue performance of ceramic package interconnections on organic laminate LCCCs.

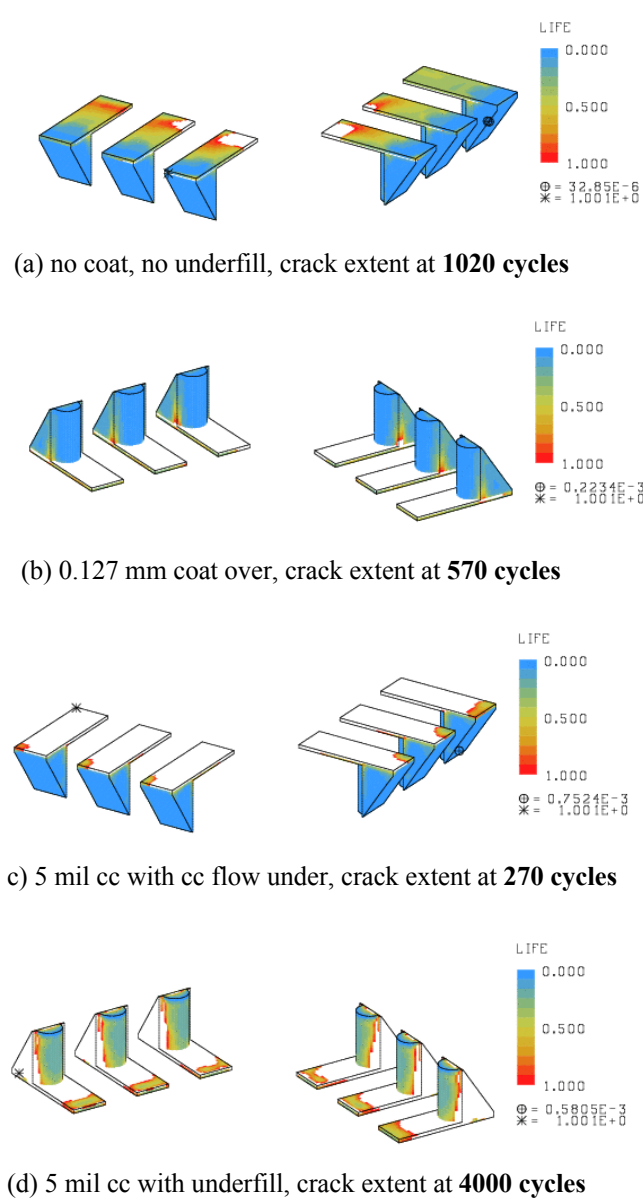


Figure 6. Predicted LCCC24 crack extent from cracking simulations. White elements are cracked.

PQFN package predictions with comparisons to the LCCC package predictions

Next, the analysis turned to the PQFN packages. The computational model predictions are shown in Figure 7 for cycles to crack initiation. In this case, the solder was void-free under the Cu paddle. The baseline condition is shown in Figure 7a. The PQFN solder joints experienced nearly an order-of-magnitude increase in the number of cycles to crack initiation versus the LCCC. Improved fatigue life was due to replacement of ceramic in the LCCC with molding compound that, together with the Cu paddle gave rise to a package CTE that was better matched to the PCB.

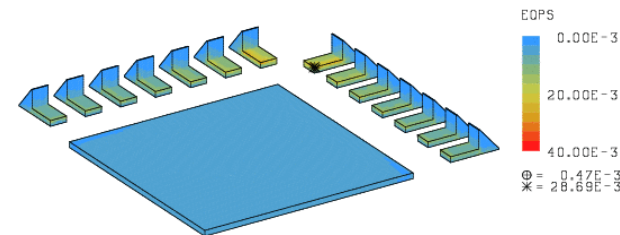
The general distribution of EQPS amongst the solder joints was the same as that observed in the baseline predictions for the LCCC package – the corner joints experienced the greatest EQPS due to having the greatest DNP as well as shear loading dominating TMF deformation. However, there was a difference in the local EQPS distribution. The element at which the TMF crack initiates in the corner PQFN joints was at the inner edge of the gap rather than at the corner of the package per the LCCC case. This behavior reflects the complex structure created by the stack of Cu paddle, Si die, and molding compound, and their different, respective modulus and CTE properties compared to the relatively homogenous LCCC package structure. The capability to predict the behavior of such a complex structure would be difficult without computational modeling.

The effect of applying conformal coating to the top of the PQFN and PCB surfaces (none in the gap) was a significant reduction in TMF cycles to crack initiation (Figure 7b). The strain contour pattern is very similar to that of the baseline case (Figure 7a), implying that the fatigue load remained predominantly shear in nature. Therefore, it appears that, like the case of the LCCC package, the coupling of the conformal coating to the PCB caused the latter to have a higher effective CTE. The consequence was a quicker path to TMF crack initiation. The fact that the percentage drop was not dramatically different from that of the LCCC case implies that the impact of the conformal coating on TMF crack initiation was proportionally the same between these two PQFN and LCCC packages, that proportion being based upon baseline TMF lifetime. Still, PQFN interconnections remained more resilient to TMF deformation that leads up to cracks owing to its unique construction.

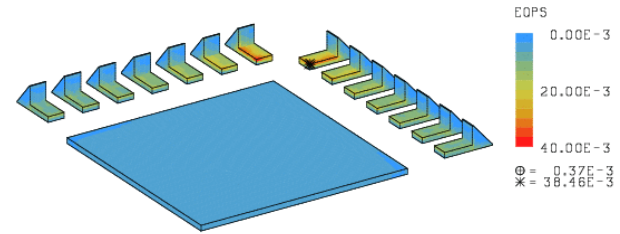
The similarity of TMF performance was most striking between the LCCC and PQFN packages when conformal coating was present in the package/PCB gap. The cycles to crack initiation dropped to 11 (Figure 7c), which was the same as the 12 cycles predicted for the LCCC (Figure 5c). This absence of a significant difference implies that the “conformal coating effect” overwhelmed any difference in the package construction. That is, the pushing-up and pulling-down of the package from the PCB surface (YY direction), which greatly accelerated the TMF of joints, did so with a similar magnitude because both package types had

similar area footprints. It is noted in Figure 7c that crack initiation also occurred along the edge of the paddle joint.

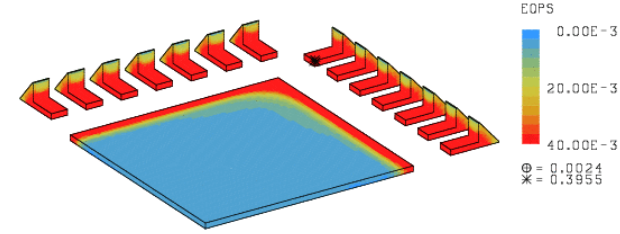
The replacement of the conformal coating between the PQFN and PCB with the underfill material mitigated the extreme loss of fatigue life with 6100 cycles predicted to crack initiation (Figure 7d). The fatigue life increased by nearly three-fold versus the baseline condition, which duplicates the proportional increase observed between the same two scenarios for LCCC package. It is interesting to note in Figure 7d that the crack initiation point has moved to the corner of the package like the case of the LCCC (Figure 5d). Assuming that its location at the pad edge in Figure 7a was due to the Cu paddle/Si die/molding compound structure, it was concluded that underfill mitigates to some extent this contribution to TMF of PQFN interconnections.



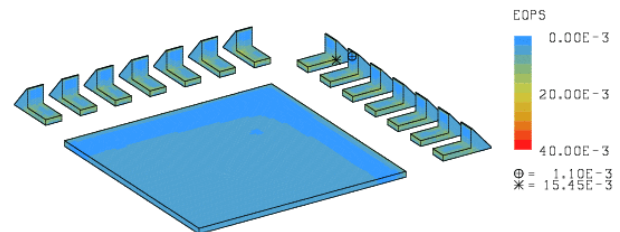
(a) no coat, no underfill 1810 cycles to start crack



(b) 0.127 mm coat over, 1020 cycles to start crack



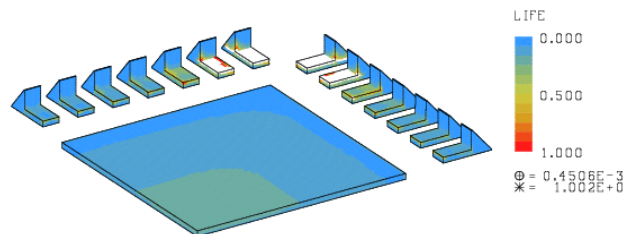
(c) 5 mil cc with cc flow under, 11 cycles to start crack



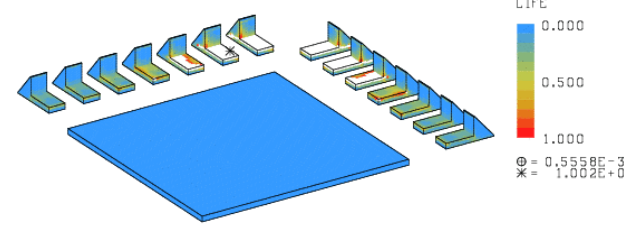
(d) 5 mil cc with underfill, 6100 cycles to start crack

Figure 7. Predicted solder Δ EQPS for 56 I/O PQFN.

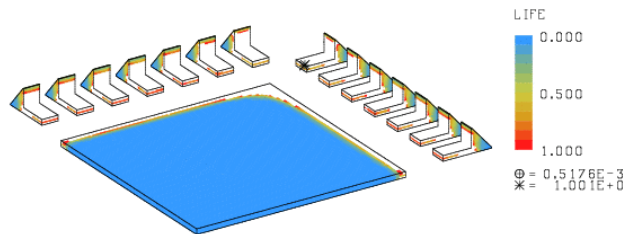
The UCPD simulation was used to predict 100% TMF crack propagation (electrical open) in PQFN solder joints. Those results are shown in Figure 8. As anticipated from the crack initiation data in Figure 7a, failure occurred at the corner joints. Beginning with the baseline case in Figure 8a, the cracks initiated at the inside edge of the pad and propagated out towards the fillet toe in nearly a straight path along the pad/fillet interface. A completely open interconnection occurred at the corner joint after 7750 cycles, which is 7.6x longer than the TMF lifetime of the LCCC package. The final failure was in the corner joint. The four corner joints experienced the greatest degree of deformation. That deformation quickly diminished for the remaining joints.



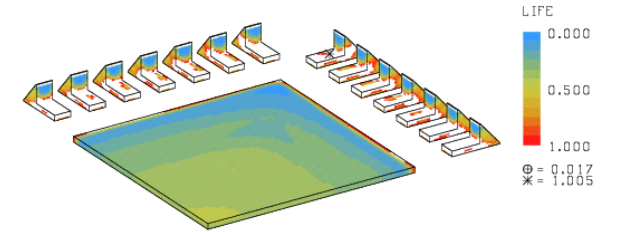
(a) no coat, no underfill, crack extent at 7750 cycles



(b) 0.127 mm coat over, crack extent at 3750 cycles



(c) 5 mil cc with cc flow under, crack extent at 160 cycles



(d) 5 mil cc with underfill, crack extent at 19,000 cycles

Figure 8. Predicted PQFN crack extent from cracking simulations.

The presence of the conformal coating over the package and PCB caused the TMF crack lifetime to decrease from 7750 cycles (baseline) to 3750 cycles (Figure 8b). The crack damage remained focused on the corner joints, affirming that the conformal coating simply accelerated the TMF cracking process by giving rise to a higher effective CTE for the PCB. The fracture morphology remained the same in those corner joints as was documented for the baseline case.

The allowance for conformal coating to flow under the package (Figure 8c) caused the same precipitous loss of TMF cycles to reach 100% crack as observed with the LCCC solder joints. The PQFN exhibited 160 cycles, which is slightly lower than the 270 cycles predicted for LCCC package. Failure occurred in nearly all of the joints, to very similar degrees. Although the conformal coating applied pressure to the package bottom, which is the same scenario as predicted for the LCCC package, there was a slight difference in the crack path. In the case of the LCCC, there was a straight crack path that remained entirely along the solder/pad interface. On the other hand, a close examination of Figure 8c shows that the failure path changed to a 45° trajectory at the corner of the PQFN package. The crack then continued along that direction through the fillet. Nevertheless, these predictions clearly show that there is no advantage gained by using the PQFN package versus the LCCC package when conformal coating is allowed between either geometry and the PCB – the conformal coating *controls* the TMF lifetime of the respective interconnections. It is also observed that cracking had begun at the corner and along the edges of the paddle solder joint.

The final case is that of placing an underfill under the PQFN in conjunction with the conformal coating over the top and on the PCB (Figure 8d). The cycles to 100% cracking occurred first in the corner joints. However, the interconnections had withstood so many cycles that all of them had reached a point of near-failure. It was interesting to note that the crack propagation path was similar to that in Figure 8c, that is, the crack path taking a 45° trajectory through the fillet after reaching the package corner from the gap. This observation implies that the PQFN and LCCC behave slightly differently under the stress conditions generated by a material between either and the PCB. Specifically, it is construed that the two packages exhibited different responses to the *pressure* placed on each by the material in the gap, whether the latter is conformal coating with a high pressure, or the underfill material with a lesser pressure.

Direct comparative analysis: LCCC versus PQFN

A direct comparison was made of the TMF behaviors between the LCCC and PQFN packages. The analysis began with the baseline condition. The cycle predictions are listed below:

- LCCC; initiation (Figure 5a): 190 cycles

- LCCC; 100% crack (Figure 6a): 1020 cycles
- PQFN; initiation (Figure 7a): 1810 cycles
- PQFN; 100% crack (Figure 8a): 7750 cycles

Point 1: Clearly, the PQFN has, in general, a greater absolute resistance to TMF than does the LCCC package. Between the two packages, the PQFN is 9.5x more resistant to TMF crack *initiation*, but only 7.1x more resistant to crack *propagation*. The cycles of crack propagation are computed by subtracting the cycles to crack initiation from the cycles to 100% crack development. The latter is a combination of cycles to initiation plus cycles causing crack propagation to an electrical open. Combining both initiation and propagation segments, the PQFN has a greater TMF lifetime by 7.6x; the crack propagation has a greater effect because it encompasses a larger percentage of the total TMF lifetime.

Point 2: LCCC: 81% of the total TMF lifetime is taken up by crack propagation while that figure is 77% for the PQFN.

The Points 1 and 2 above confirm that there is a difference, albeit relatively small, between the *baseline* TMF performances of the two packages.

The same analysis was performed when there is the presence of both conformal coating *and* underfill. The cycle predictions are listed below:

- LCCC; initiation (Figure 5d): 640 cycles
- LCCC; 100% crack (Figure 6d): 4000 cycles
- PQFN; initiation (Figure 7d): 6100 cycles
- PQFN; 100% crack (Figure 8d): 19,000 cycles

Clearly, a comparison of these results and those of the baseline confirmed that the underfill not only prevented the deleterious effects of conformal coating flowing into the package/PCB gap, but it also enhanced the TMF resistance of the solder joints for both package types. The PQFN remains 9.5x more resistant to TMF crack *initiation*, which is similar to the baseline case. But, the PQFN solder joints were only 3.8x more resistant to crack propagation than the LCCC interconnections, which is about one-half of the multiplier observed in the baseline condition, above. Further analysis of the model predictions indicated that the difference is due to the fact that the underfill improved the TMF of the LCCC solder joints nearly two-fold *more so*, than it did for the PQFN solder joints. Moreover, because crack propagation is such a significant portion of the overall TMF lifetime of the interconnections, a similar trend is observed when comparing 100% crack predictions: 19,000 cycles (PQFN) to 4000 cycles (LCCC). Those values differ by a factor of 4.8x versus 7.6x for the baseline condition. Therefore, the introduction of the underfill improved the TMF resistance of both packages; however it was more effective for the LCCC package and, specifically, in the crack propagation segment of their fatigue lifetime.

Effect of paddle voids on predicted TMF of PQFN

The computational model was exercised whereby the paddle solder joint had a 30% void content (Figure 2g). The EQPS predictions of crack initiation are shown in Figure 9 for the four cases, beginning with the baseline (no conformal coating; no underfill) that is shown in Figure 9a. These results were compared to those in Figure 7a (no voids). The predicted cycles to crack initiation with voids, 1731 cycles, are similar to the cycle count without voids, 1810 cycles.

The very same trends were observed in the remaining three cases: conformal coating only, Figure 9b; conformal coating under the PQFN, Figure 9c; and conformal coating plus underfill, Figure 9d, all predicted similar cycles to crack initiation as the corresponding, no-void cases in Figure 7.

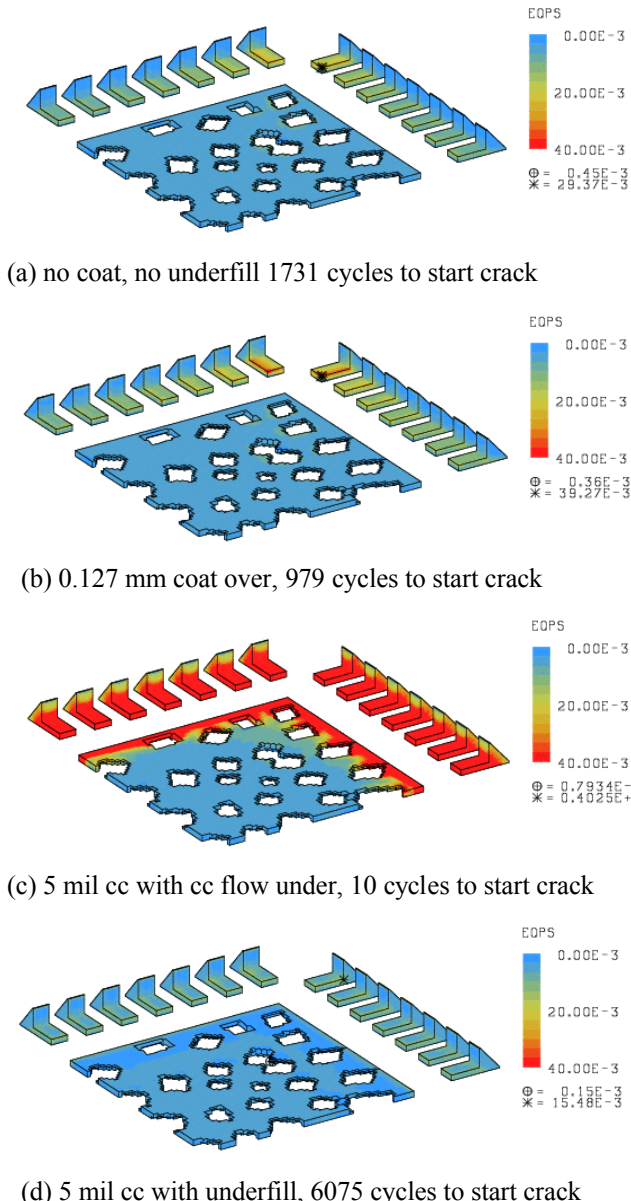


Figure 9. Predicted solder Δ EQPS for 56 I/O PQFN with 30% voids in the paddle joint

It is particularly interesting to compare Figures 7c and 9c, which represent the no-void and 30% void cases, respectively, when conformal coating filled the gap under the package. This scenario is the most severe condition as illustrate by the very few cycles (10 – 11) and is most likely to contrast the different void scenarios. Yet, the colored EQPS contours between these two figures illustrate the point that the presence of voids did not affect the TMF behavior of the paddle solder joint.

The crack simulation (UCPD) model was applied to the case of voids in the paddle solder joint. A comparison was made between Figure 8 (no voids) and Figure 10 (30% voids).

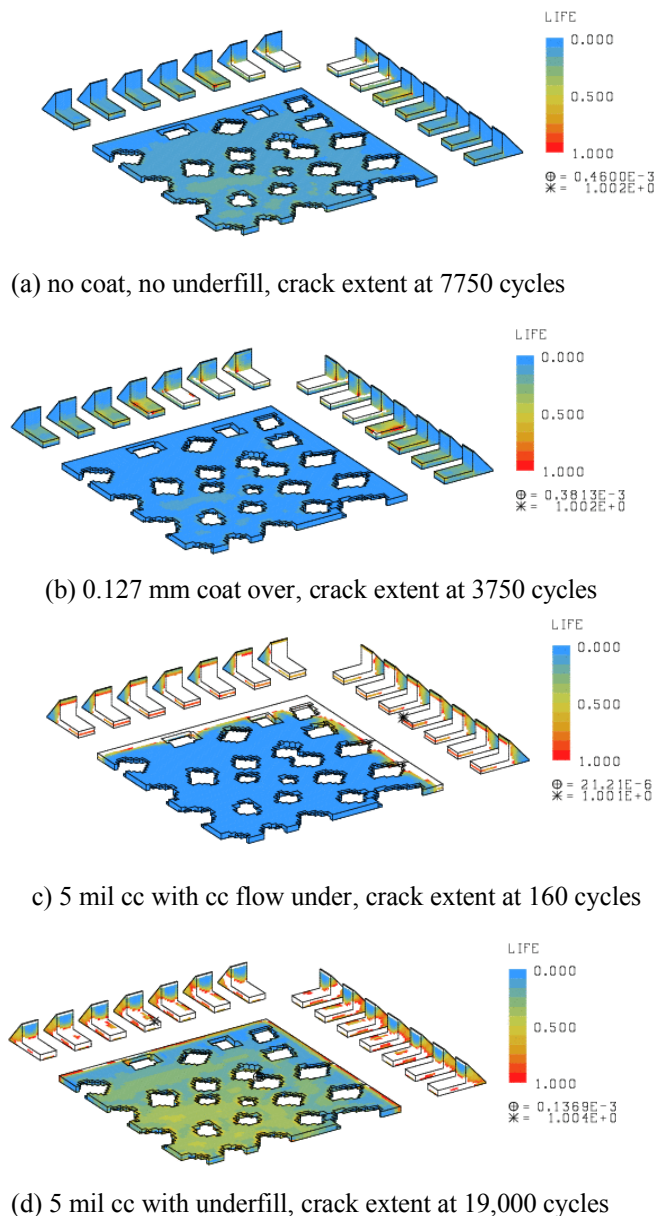


Figure 10. Predicted PQFN with voids crack extent from cracking simulations.

The predicted cycles to 100% cracking as well as the crack paths were identical between the two cases. The voids did not affect the TMF crack behavior of the peripheral solder joints. The worst-case of TMF cracking – conformal coating in the gap – was examined between Figures 8c and 10c with respect to cracking of the paddle solder joint. There was only a slightly greater degree of crack propagation into the paddle joint having 30% voids than was observed in the non-void containing joints. In Figure 10c, the crack had begun to encroach into the voids. The resulting stress concentrations near those voids slightly accelerated localized crack growth that, in turn, allowed for a small increase in crack propagation everywhere else along the front when compared the case when voids were absent. Nevertheless, the paddle crack growth was sufficiently small that it would *not* jeopardize the reliability of the large paddle solder joint with respect to either electrical or thermal management functions.

SUMMARY

The numerical predictions have been summarized in Table 4 to assist the reader with understanding the important findings described below:

1. High reliability systems are looking to the commercial electronics supply chain to provide advanced packages that meet the goals of reducing size, weight, and power (SWaP) requirements.
2. It is necessary to assure that these new package concepts also provide for second-level interconnections that meet stringent reliability specifications.
3. In light of program constraints on budget and schedule, design engineers are relying heavily on computational modeling to predict the reliability of solder joints as an alternative to expensive, time-consuming experimental programs.
4. The Sandia solder fatigue computational model was used to predict the effects of conformal coating and underfill on the thermal mechanical fatigue (TMF) reliability of 63Sn-37Pb (wt.%) solder joints formed between a 56 I/O plastic quad-flat, no-lead (PQFN) package and a 2.36 mm thick, polyimide glass printed circuit board (PCB). The analysis included the traditional 24 I/O leadless ceramic chip carrier (LCCC) package of similar footprint size.
5. Model predictions were made for an accelerated aging thermal cycle of -55°C/85°C. Hold times were 90 min at the temperature extremes. Two failure criteria were used: (a) cycles to crack initiation and (b) cycles to cause 100% cracking (electrical open) of a solder joint.
6. As expected, the LCCC experienced a considerably shorter baseline, TMF lifetime than did the PQFN.
7. Placing a conformal coating over the PWA reduced the TMF lifetime of both components in similar proportions to their baseline values because the coating caused a greater, effective CTE to the PCB that enhanced the shear loads introduced to the solder joints.
8. Having the conformal coating flow into the package/PCB gap caused a significant drop of TMF lifetime (crack initiation, 100% crack) to (12 cycles,

270 cycles) for the LCCC and (11 cycles, 160 cycles) for the PQFN. The lower lifetimes reflected the similar magnitude of coat pressure applied to package bottom that was the primary source of TMF deformation.

9. The introduction of the underfill material not only prevented the deleterious effects on TMF caused by incursion of conformal coating under the package, but also enhanced the TMF lifetimes of both packages above their baseline values.
10. The presence of 30% voids in the paddle joint of the PQFN had negligible effect on the TMF lifetimes of the peripheral solder interconnections. However, there was a slight enhancement of crack propagation in the paddle solder joint.

Table 4. Predicted cycles to fatigue crack start and open.

Model	ΔEQPS	Cycles to Start Crack	Cycles to Electrical Open
LCCC24			
LCCC24_free	0.090650	189.9	1020
LCCC24_cc	0.117800	113.6	570
LCCC24_cc under	0.375400	11.7	270
LCCC24_ufill	0.048900	636.9	4000
QFN56			
qfn56_free	0.028690	1811.8	7750
qfn56_cc	0.038460	1019.9	3750
qfn56_cc under	0.395500	10.6	160
qfn56_ufill	0.015450	6097.9	19000
QFN56 voids			
qfn56_free	0.029370	1730.5	7750
qfn56_cc	0.039270	979.0	3750
qfn56_cc under	0.402500	10.2	160
qfn56_ufill	0.015480	6074.7	19000

ACKNOWLEDGEMENTS

The authors wish to thank Dr. Edward Russick for performing Young's modulus measurements of conformal coat and underfill materials as well Don Susan for his thorough review of the manuscript. Sandia National Laboratories is a multiprogram laboratory managed and operated by Sandia Corporation, a wholly owned subsidiary of Lockheed Martin Corporation, for the U.S. Department of Energy's National Nuclear Security Administration under Contract No. DE-AC04-94AL85000.

REFERENCES

- [1] M.K. Neilsen and P.T. Vianco, 'UCPD Model for Pb-Free Solder,' *J. Electronic Packaging*, Vol. 136, Dec. 2014
- [2] H.D. Solomon, 'Fatigue of 60/40 Solder,' *IEEE Trans. on Components, Hybrids, and Manufacturing Technology*, Vol. CHMT-9, No. 4, December 1986.